Organic & Biomolecular Chemistry

Side-chain deuterated cholesterol as a molecular probe to determine membrane order and cholesterol partitioning

Journal:	*Organic & Biomolecular Chemistry*
Manuscript ID	OB-ART-06-2019-001342.R2
Article Type:	Paper
Date Submitted by the Author:	05-Sep-2019
Complete List of Authors:	Hanashima, Shinya; Osaka University, Department of Chemistry Ibata, Yuki; Osaka University, Department of Chemistry WATANABE, Hirofumi; Osaka University, Department of Chemistry Yasuda, Tomokazu; Osaka University, Graduate School of Science Tsuchikawa, Hiroshi; Osaka University, Graduate School of Science, Department of Chemistry Murata, Michio; Osaka University, Graduate School of Science

Side-chain deuterated cholesterol as a molecular probe to determine membrane order and cholesterol partitioning

Shinya Hanashima*, Yuki Ibata, Hirofumi Watanabe, Tomokazu Yasuda, Hiroshi Tsuchikawa, Michio Murata*

Department of Chemistry, Graduate School of Science, Osaka University, Machikaneyama1-1, Toyonaka, Osaka 560-0043, Japan

*Corresponding author to be addressed;

e-mail; hanashimas13@chem.sci.osaka-u.ac.jp; murata@chem.sci.osaka-u.ac.jp

Abstract

Cholesterol is an essential and ubiquitous component in mammalian cell membranes. However, its distributions and interactions with phospholipids are often elusive, partly because chemical modifications for preparing cholesterol probes often cause significant perturbations in its membrane behavior. To overcome these problems, a ^{2}H-labeled probe (24-*d*-cholesterol), which perfectly retained the original membrane properties, was synthesized by a stereoselective introduction of ^{2}H into the side chain of cholesterol. A deuterium label at the side-chain more sensitively reflects membrane fluidity than the conventional labeling at the 3 position of a sterol core (3-*d*-cholesterol), thus providing 24-*d*-cholesterol with desirable properties to report membrane ordering. Solid state ^{2}H NMR of 24-*d*-cholesterol with sphingomyelins (SM) and unsaturated phosphatidylcholine in the bilayer membranes clearly revealed the partitioning ratio of cholesterol in the rafts-like liquid ordered (Lo) phase and the liquid disordered phase based on cholesterol interactions with lipids in each phase. This probe turned out to be superior to the widely used 3-*d*-cholesterol; e.g., 24-*d*-cholesterol clearly revealed a 10 mol% difference in the Lo distribution ratios of cholesterol between palmitoyl-SM and stearoyl-SM. The comprehensive use of 24-*d*-cholesterol in solid state ^{2}H NMR will disclose the cholesterol-lipid interactions, distribution ratio of cholesterol, and membrane ordering in model bilayers as well as more complicated biological membranes.

Introduction

Cholesterol (Cho) is an indispensable lipid in vertebrate cells consisting of 20–25% of the total lipids in the plasma membrane. Cho is involved in the formation of the biologically functional domain called lipids rafts along with sphingomyelin (SM) and other glycosphingolipids.[1,2] In model bilayer membranes, the interactions with SMs induce the liquid-ordered (Lo) phase[3-5] by increasing membrane ordering through the hydrophobic interaction between the rigid sterol core of Cho and the saturated acyl chain of sphingolipids,[6-8] which is known as the Cho condensing effect.[9] The SM-Cho interaction in membranes is known to alter the binding amount of the SM binding proteins on the membrane surfaces.[10-12]

Cho distribution and interactions in cell membranes and model membranes are key issues that need to be clarified.[13] Filipin, a polyene antibiotic,[14] perfringolysin O and related bacterial proteins targeting the Cho,[15] and NBD-tagged and Bodipy-tagged Cho derivatives[16] have been widely used for this purpose; however, the lipid organization in membrane are perturbed,[17] Lo to Ld phase partition coefficients of such fluorescent Cho probes are significantly different from Cho itself because of the large fluorescence moieties at the side chain,[18,19] the binding proteins often affect the Cho dynamics,[20] and even the trace amounts (< 1 mol %) of these probes often perturb the morphology of the micro- and nanodomains.[21] Fluorescent Cho analogues cholestatrienol and dehydroergosterol are useful mimics used for detecting membrane distribution, biophysical properties, and the transport of Cho.[22-24] Although structurally similar analogues mimicking the Cho's membrane properties are often used for studying biological and artificial membranes,[25] serious limitations, such as perturbations in membrane behavior, lower ordering effect, the short excitation wavelength, and the weak

fluorescence intensities, have hampered broad applications.[22,26] Cho probes carrying a stable N-oxyradical have been used for electron paramagnetic resonance (EPR) and fluorescence quenching experiments, although the ordering effect was weaker than that of Cho.[27] A recent technique using imaging MS directly shows Cho distribution in planer monolayers in a quantifiable manner.[28]

The hydrophobic moiety of SM, which plays a key role in SM-Cho interactions, consists of a sphingosine chain and a fatty acyl chain. SM bearing a palmitoyl group (C16:0, PSM in Fig. 1) is normally a major sphingolipid in the plasma membrane of the mammalian cells,[29-31] while some tissues, including the brain and skeletal muscles, contain more SM bearing a stearoyl chain (C18:0, SSM in Fig. 1).[32] The characteristic distribution may partly account for the expression pattern of the six ceramide synthases, which have individual preferences for the substrate chain length of the CoA-linked fatty acids.[33,34] However, it is largely unclear why SSM and PSM distribute quite differently in tissues and organelles.

Solid state ^{2}H NMR is a sensitive method to examine the lipid interactions by measuring the mobility of the deuterated lipids in bilayers.[35] The width of the Pake doublet ($\Delta\nu$) obtained from ^{2}H NMR spectra clearly reveals the degree of wobbling of a deuterated segment. In ternary membrane systems with co-existing Lo and Ld phases, the deuterated lipid usually causes two sets of Pake doublets originating from the partitioning to the Lo and the Ld phases respectively through the preferable and disfavored lipid interactions.[36,37] Thus, we have been developing deuterated probes of phospholipids such as 10'-d_2-SSM[37] and 6'-d_2-DOPC[38] for the analysis of lipid ordering and partition. The 3-deuterated Cho (3dCho) has been widely used as a ^{2}H NMR probe to examine Cho interactions[39] and Lo/Ld distributions[37,40] in lipid bilayers; however, differences in the

Pake doublet widths between the Lo and Ld phases is small because the deuterated position is located in the rigid sterol core, which does not sharply reflect the wobbling effects of surrounding hydrocarbon chains of lipids. It is reported that the doublet widths are more significantly influenced by the tilt angle of the rigid sterol ring system in phospholipid membranes.[41] Therefore, a Cho probe with deuteration at the flexible side chain is expected to better reflect the membrane ordering and the Lo/Ld distributions of Cho. Actually, Cho carrying multiple deuterations at the flexible side chain (C22-C27) is known to be highly susceptible to the order of surrounding lipids;[42] however, the multiple deuteration sites cause the signals to have heavy overlapping, which hampers the quantifiable spectral analysis necessary to determine the partition ratios of Cho between the Lo and Ld phases.

In this study, a novel deuterated Cho with a single deuterium atom at the 24(*S*) position (24dCho) was designed and synthesized (Fig. 1). This position on the flexible side chain is expected to be sensitive to the ordering effects from the surrounding lipids, thus provides a large difference in the quadrupole splitting between the Lo and Ld phases,[42] which greatly facilitates accurate determination of the Cho partition rate by measuring the peak areas for the well separated ^{2}H signals from each phase. In addition, perturbations in membrane physicochemical properties by the single deuterium substitution are negligible. Cho exists as a single molecular species in the plasma membrane, while glycerolipids and sphingolipids are highly diverse in their head groups, length of the hydrocarbon chains with or without double bonds. Therefore, deuterated Cho could be an ideal molecular sensor to comprehensively compare the physicochemical properties of lipid membranes including model bilayers and plasma membranes by means of solid state ^{2}H NMR.

First, the diastereoselective synthesis of 24dCho was achieved. With the compound thus obtained, its utility as an NMR probe was examined by evaluating the lipid interactions with SMs and determining the Lo/Ld partition ratios of 24dCho for two similar Lo/Ld coexisting systems. SSM/DOPC/Cho and PSM/DOPC/Cho bilayers were the focus because SSM has been reported to have a slightly lower affinity to Cho than PSM;[43] however, the Cho probe, which is partitioned significantly higher to the Lo phase of the SSM bilayers than to that of the PSM bilayers despite the difference between SSM and PSM, was only in the acyl chain length by one ethylene segment. Therefore, 24dCho was proven to be an excellent probe to precisely measure Lo/Ld partition ratios of Cho.

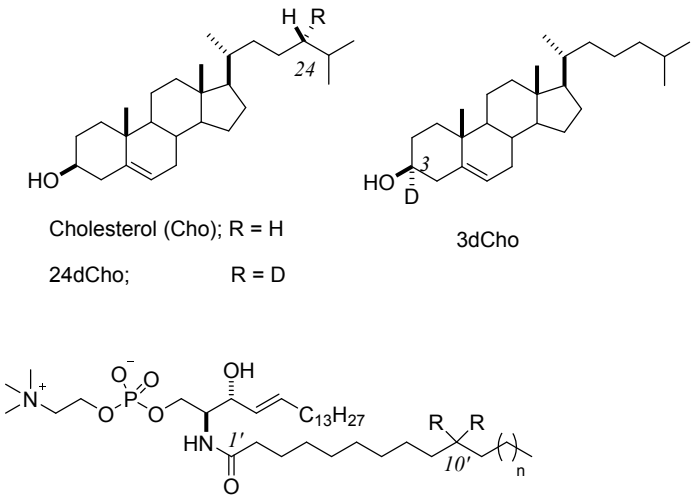

Figure 1. Structures of 24dCho, 3dCho, and SMs. d_2-SSM has two deuterium at the 10' position of the acyl chain.

Results and Discussion

Design and Synthesis of 24dCho

The C24 methylene is expected to be one of the ideal positions to sensitively reflect the ordering of surrounding lipids. A labeled position should not be influenced by a rigid sterol core since the tetracyclic core sometimes alters its orientation by interacting with surrounding lipids, which prevents the selective observation of the acyl chain ordering by ^{2}H NMR. The C24 position is less susceptible to the orientation change because it is separated from the core by a C_3 chain, which is grossly in the extended conformation.[42] It is also expected that the terminal isopropyl group, C25/C26/C27, is not desirable because of its conformational ambiguity in bilayers and also the narrow splitting width of ^{2}H signals.[42]

The synthesis of 24dCho was achieved in seven steps from commercial 3β-hydroxy-Δ5-cholenic acid. Initially, deuterated aldehyde **4** was prepared in three steps.[44] The hydroxy group of 3β-hydroxy-Δ5-cholenic acid was protected by a TBS group, and following reduction using $LiAlD_4$, it produced deuterated alcohol **3** in a moderate yield. The PCC oxidation of **3** provided deuterated aldehyde **4** in 54% yield. Then, the diastereoselective reduction of the deuterated aldehyde **4** was achieved under Midland reduction conditions using (*R*)-alpine borane[45] to produce the desired alcohol **5** in 96% yield (> 95% d.e.). The stereochemistry at the C24 position was determined to be the *S* configuration by the Mosher method through the derivatization of an aliquot of **5** into an MTPA ester (Fig. S1).[46] Then, the treatment of **5** with CBr_4 and Ph_3P produced bromide **6** in 70% yield. The terminal isopropyl group was introduced to the bromide **6** by treatment with *i*-PrMgBr and Li_2CuCl_4, and following deprotection, it produced the desired 24dCho **1** in 82% yield (2 steps). The stereochemistry of the deuterium at C24 was confirmed through the comparison of the ^{1}H NMR chemical shifts of the remaining ^{1}H at C24 with non-

labeled Cho (Figs. 2 and S2).[47] A cross peak in HSQC due to the remaining 24*R*-H versus C24 of 24dCho was found at 1.07 and 39.1 ppm, respectively, where a triplet was observed along the ^{13}C axis due to the geminal ^{13}C-^{2}H coupling ($^{1}J_{C\text{-}D}$ = 17.1 Hz), while the signal at pro-chiral 24*R* and 24*S* were found in 1.09 ppm and 1.11 ppm in Cho. The chemical shifts differences along both ^{1}H and ^{13}C axes can be accounted for by deuterium-induced isotope shifts (DIS), which is in the range from −0.01 to −0.02 ppm.[48] Thus, the stereochemistry at C24 was identified to be *S* as expected from the stereochemical preference of the reaction. Prior to use for the membrane experiments, **1** was further purified by HPLC under reverse phase conditions (column; ODS, solvent: MeOH).

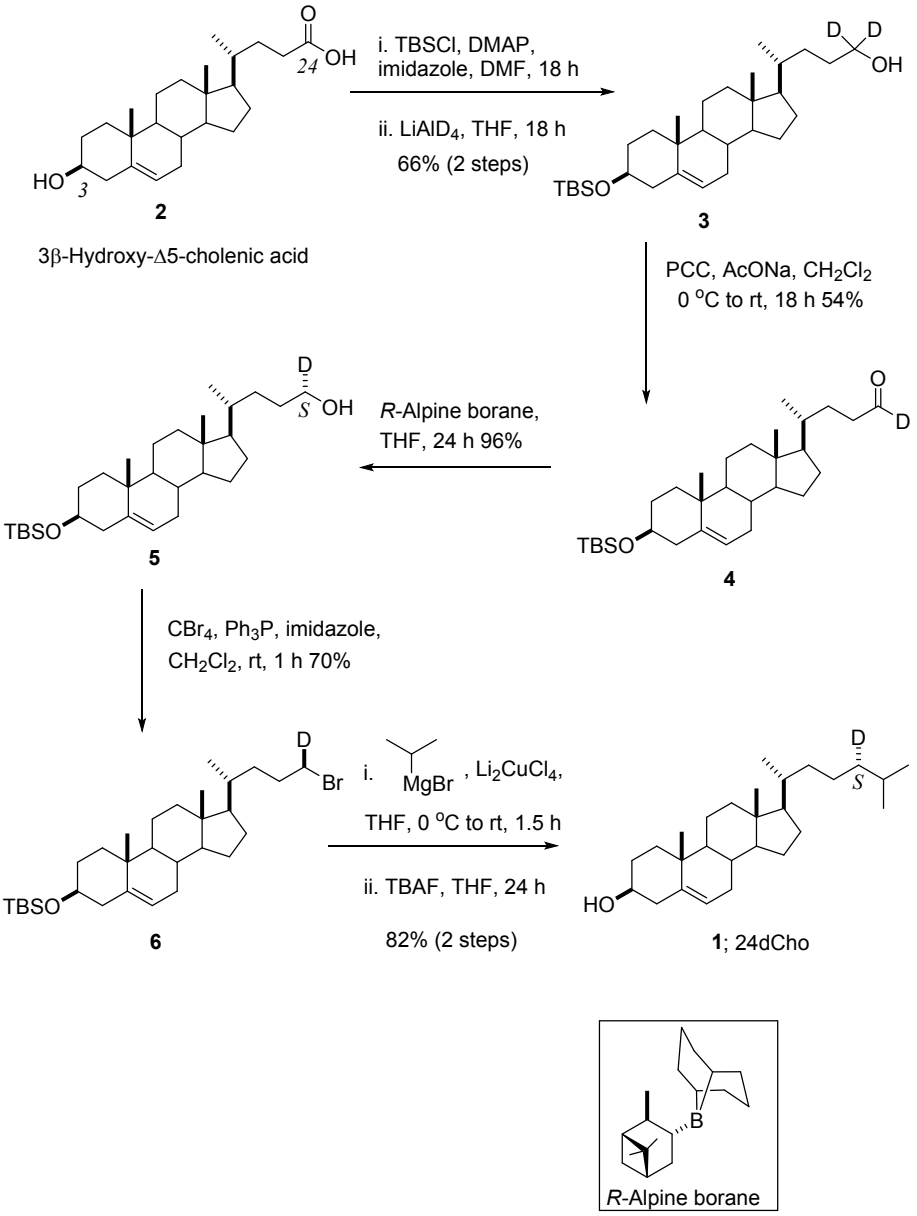

Scheme 1. Synthesis of 24dCho **1**.

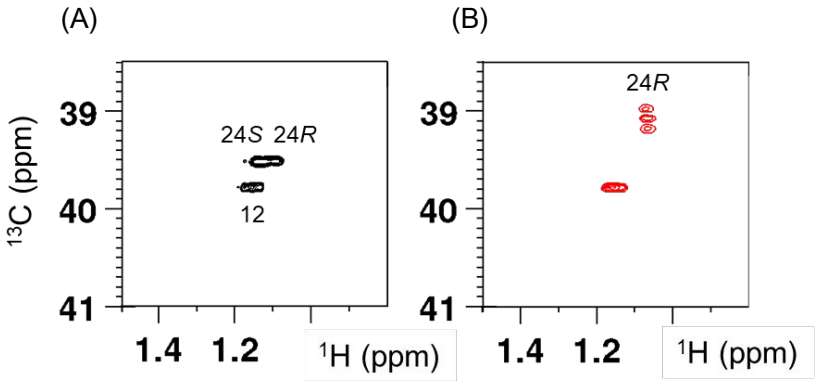

Figure 2. Comparison of the ^{1}H-^{13}C HSQC spectra of Cho (A) and 24dCho (B) in $CDCl_3$. See also Fig. S2. in Supporting Information.

Solid state ^{2}H NMR of 24dCho in binary SM/Cho bilayers

Cho is known to alter the SM bilayer from the highly packed gel phase or the Ld phase to the Lo phase through SM-Cho interactions.[5,49] To demonstrate whether the ^{2}H NMR signal of 24dCho highly reflects the mobility of surrounding hydrocarbon chains due to lipid interactions, a binary SM/Cho bilayer system in a multi lamellar vesicle (MLV) was first employed. Pake doublet width ($\Delta\nu$) of d_2-SSM (Fig. 1), which has ^{2}H-labeling in the middle part of an acyl chain, was compared with those of 24dCho and 3dCho. In the solid-state NMR of the d_2-SSM, the ordering effect of Cho on the acyl chain is shown by a marked increase in the Pake doublet width ($\Delta\nu$).[50] Actually, the 10' position of the SM acyl chain, where it is highly susceptible to the Cho ordering effect,[7] shows the $\Delta\nu$ value of 53.3 kHz (30 °C) in SSM/Cho 8:2 bilayers (Fig. 3A). According to the phase diagram,[51] the SSM/Cho membrane probably undergoes the Lo and gel coexisting phase at 30 °C. Therefore, the ^{2}H NMR spectral shape in Fig3A was distorted because the fluidic Lo

phase provided the doublet in 53.3 kHz and the rigid gel phase provided broaden components. The $\Delta\nu$ value of the lipid hydrocarbon chains in the presence of Cho gradually decreases as the temperature rises from 53.3 through 49.2 to 43.1 kHz at 30, 40, and 50 °C, respectively (Fig. 3A, Table 1). The spectral shape at 40 °C indicates that the gel phase almost disappears and shifts to the Lo phase. The Lo phase was preserved up to the melting temperature of SSM (T_m; 44.8 °C).[52] The 3dCho in the same system (SSM/3dCho 8:2) did not clearly show temperature-dependent changes of the Δν values (Fig. 3B), which is a sharp contrast to the d_2-SSM. The Δν value of 45.2 kHz with a broadened component at 30 °C was slightly increased to 46.9 kHz at 40 °C and then decreased to 43.5 kHz at 50 °C. These Δν differences on the temperature independent change, particularly under T_m, originates from the restricted mobility of the deuterium on the steroidal core. In sharp contrast, 24dCho clearly showed a temperature-dependent decrease of the Δν values in the same membrane system (SSM/24dCho 8:2) (Fig. 3C). The Δν values were 36.3 kHz at 30 °C and decreased to 34.4 kHz (40 °C) and then to 27.8 kHz (50 °C). It is clear that 24dCho is superior than 3dCho to monitor the membrane ordering in melting of SM because of the decrease in the relative Δν values similar to d_2-SSM (Fig. S7). The smaller Δν values compared to that of d_2-SSM is probably due to the difference in the membrane depth of the deuterated carbon.[7] A similar temperature-dependent decrease was also observed for the PSM/24dCho 8:2 system (Table 1). In this PSM bilayer, the Δν values were 35.0, 32.7, and 27.0 kHz at 30 °C, 40 °C, and 50 °C, respectively; the difference in the melting temperatures between PSM (41.0 °C)[52] and SSM only slightly affected the Δν values. Thus, the data demonstrate that 24dCho accurately reflects the mobility change of the surrounding lipid, shown as the Δν values of d_2-SSM, compared with 3dCho. The trends in decreasing Δν values of 24dCho were

comparable to the decrease of the fluorescent anisotropy using diphenylhexatriene, which is good reporter for membrane fluidity (Fig.S8).

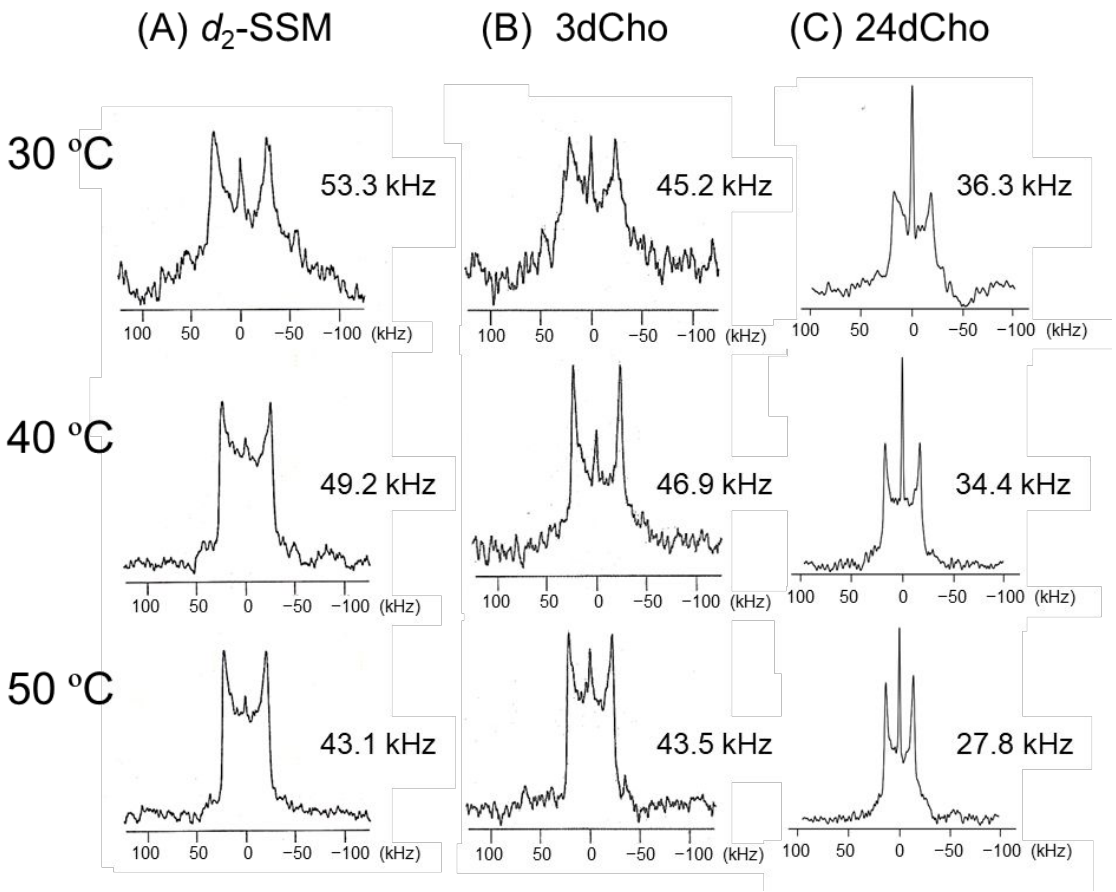

Figure 3. ^{2}H NMR spectra of the deuterated lipids in SSM/Cho 8:2 membranes at 30, 40, and 50 °C. Deuterated lipids, d_2-SSM (A), 3dCho (B), or 24dCho (C), were used instead of natural lipids. The spectra of d_2-SSM are those in our previous report.[50] The sharp center peak of the spectra originated from residual DOH. Reprinted (panel A) with permission from Langmuir, 2015, 108, 2502-2506. Copyright 2015 American Chemical Society.

Table 1. The Δν values (kHz) of the deuterated lipids in solid state ^{2}H NMR in SSM/Cho 8:2 or PSM/Cho 8:2 bilayers.

SM/Cho 8:2	deuterated lipid	Δν (kHz)		
		30 °C	40 °C	50 °C
SSM/Cho	d_2-SSM	53.3	49.2	43.1
	3dCho	45.2	46.9	43.5
	24dCho	36.3	34.4	27.8
PSM/Cho*	24dCho	35.0	32.7	27.0

*The spectra of PSM/24dCho 8:2 are shown in Supporting Information.

Solid state ^{2}H NMR of 24dCho in ternary bilayers

To demonstrate that the Cho probe efficiently exhibits Cho distribution under Lo/Ld phase separation conditions, 24dCho was mixed into the ternary SM/DOPC/Cho bilayers. The molar ratio of Cho present in the Lo and Ld phases can be determined from the peak areas of the two sets of the 24dCho signals, which create larger and smaller widths of Pake doublets, respectively.[37,40] Due to the significant differences in the Lo/Ld membrane orders, the widths of Δν in the Lo phase is much larger than that in the Ld phase.

To fulfill a macroscopical Lo/Ld phase segregation, the ternary membrane consisting of SSM/DOPC/24dCho 33:33:33[53] was selected and subjected to ^{2}H NMR measurements at 30, 40, and 50 °C (Fig. 4B). As a result, two sets of Pake doublets with the splitting widths of 35.6 kHz and 19.2 kHz, respectively, were clearly observed at 30 °C. Taking into account the membrane order, the outer doublet is 24dCho in the more ordered Lo phase, and the inner doublet originates the 24dCho in the Ld phase. Importantly, the Δν difference of 24dCho between the Lo and Ld phases was significantly larger than that of 3dCho (Lo; 47.3 Hz, Ld; 42.6 kHz) under identical conditions[37] (Fig. 4A). After increasing the temperature to 40 °C, only a single set of Pake doublets with 26.7 kHz was

observed from 24dCho. The temperature was found to be beyond the limit of the two liquid-phase coexisting conditions, thus exhibiting one coalesced Pake doublet from a mixed phase, which is consistent with the phase diagram reported for giant unilamellar vesicles.[54]

The temperature dependent Lo-Ld partition of Cho was also examined for a PSM system (PSM/DOPC/24dCho 33:33:33) (Fig. 4C). The boundary temperature between Lo-Ld phase co-existence and a mixed phase was similar to the SSM/DOPC/Cho system, creating two doublets from the Lo phase (33.4 kHz) and from the Ld phase (20.1 kHz) at 30 °C, and only one Pake doublet from a mixed phase at 22.0 kHz was observed at 40 °C.

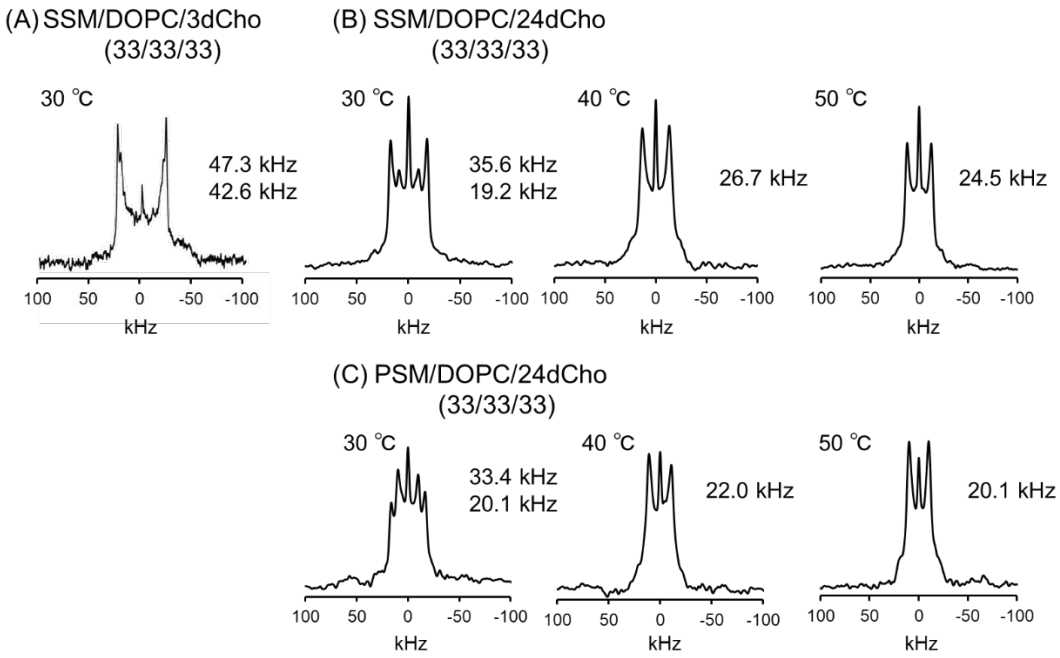

Figure 4. ^{2}H NMR spectra of SSM/DOPC/3dCho 33:33:33 membrane (A);[37] SSM/DOPC/24dCho 33:33:33 membrane (B); and PSM/DOPC/24dCho 33:33:33 membrane (C) at 30, 40, and 50 °C. Reprinted (panel A) with permission from Biophysical Journal, 2015, 31, 13783-13792. Copyright 2015 Elsevier.

The widths of the Pake doubles of 24dCho in the homogeneous phase at 40 °C showed a significant difference between the ternary SSM and PSM bilayers (Fig. 5). The differences could have originated from the structural difference of PSM and SSM, namely two-methylene gaps between the palmitoyl (16:0) and the stearoyl (18:0) chains. The difference in the Δν values at 40 °C is suggested that the longer acyl chain of SSM can transfer the ordering effect to the deeper area of the bilayer where C24 of Cho is located.

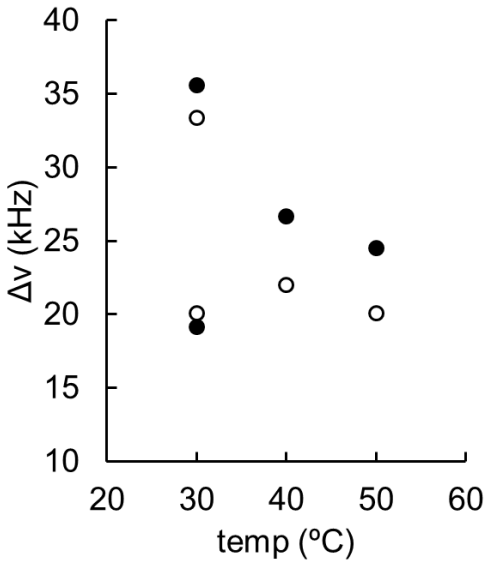

Figure 5. Summary of the temperature-dependent Pake doublet widths (Δν) of 24dCho in the SSM/DOPC/Cho 33:33:33 membrane (●) and the PSM/DOPC/Cho 33:33:33 membrane (○).

Molar fractions of Cho in SSM/DOPC/Cho bilayers

The molar fractions of deuterated lipids in the Lo and Ld phases were previously determined using ^{2}H NMR spectra.[37,40] According to the procedure, the 24dCho distribution ratios in the Lo and Ld areas were determined based on the peak areas of ^{2}H NMR signals (Fig. 6A,B).

In the SSM/DOPC/Cho 33:33:33 bilayer at 30 °C, 81 mol% and 19 mol% of 24dCho were partitioned to the Lo and the Ld phases, respectively (Fig. 6C), which was quite similar to previous results for the same bilayer system using 3dCho.[37] The use of PSM instead of SSM for the ternary SM/DOPC/Cho bilayer resulted in a 11 mol% reduction of the partition of 24dCho to the Lo phase. The difference of a two-methylene length in an SM acyl chain significantly affected the Cho partition ratio between the Lo and Ld phases. In bilayers with a lower Cho content (SSM/DOPC/24dCho 40:40:20), the partition ratio of 24dCho to the Lo phase was decreased to 73 mol% (Fig. 6D), indicating that Cho content affects the Lo/Ld partition ratio. The use of PSM instead of SSM, Cho's partition in the Lo phase, was observed in 62 mol% for the same SM/DOPC/Cho compositions. The mol% ratio of Cho in the Lo phase was again decreased relative to the SSM/DOPC/Cho membranes. Based on the previous phase diagram, the SM/DOPC/Cho 40:40:20 membrane was in the So/Lo/Ld three phase co-existing area at 30 °C.[53] Thus, a part of SM forms the gel phase through a potent SM-SM interaction,[8] and the available SM used to form the Lo phase with 24dCho was lower for the 20 mol% Cho condition. The probe in phase separated ternary lipid systems clearly reflects the ordering of surrounding lipids in the Lo and Ld phases, which allowed for accurately determining the Lo/Ld partition ratio of Cho.

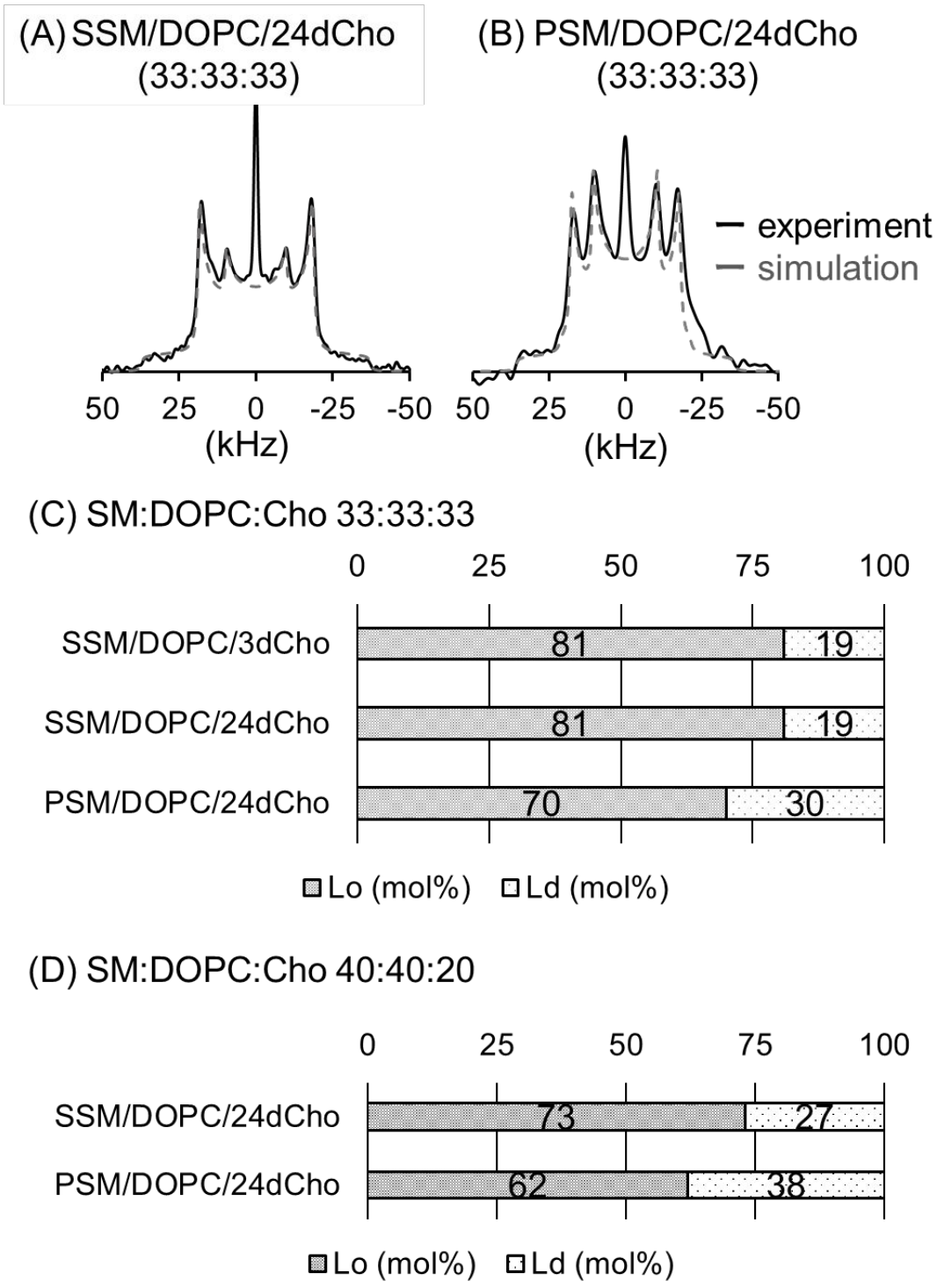

Figure 6. Cho molar fractions in the Lo and Ld phases of the SM/DOPC/Cho membrane at 30 °C. A, B; spectral fittings of the SSM/DOPC/Cho and PSM/DOPC/Cho

bilayers between the experimental spectra (black trace) and the theoretical curve (gray dashed trace). C, D: Cho mol% in the Lo (gray mesh) and Ld (white dot) phases using 24dCho in SM/DOPC/Cho 33:33:33 and 40:40:20 membranes. The Lo/Ld ratio using 3dCho was taken from a previous report.[37]

Discussion

It has been demonstrated that synthetic 24dCho is a superior NMR probe to 3dCho for determining the partition ratios of Cho in SM model membranes. In the solid state ^{2}H NMR of membrane lipids under the conditions of the axial symmetric rotation, the Δν values can be expressed by the product of the molecular order parameter S_{mol} and the averaged angular terms $<(3\cos^2\theta'-1)/2>$, where θ' is the angle between the molecular axis and the C-D vector and the angle brackets show the motional average. On the Cho structure, a C-D bond at the 3-axial position on a sterol core has a constant $\theta' = 80°$,[41] while a C-D bond at the 24 position resides in the flexible ensemble of the side chain, thus reflecting surrounding chain fluctuations and ordering effects to a much greater extent.[50] The usefulness of similar design on the deuterated position has been also proved for the phosphatidylcholine bearing unsaturated fatty acids.[38] Therefore, 24dCho, which can be stereoselectively synthesized in only seven steps, could be a more ideal probe to report the Cho-lipid interactions and Cho distribution in the Lo and the Ld phases by measuring ^{2}H NMR. As shown in the spectrum of 3*d*Cho in Fig. 5A, the difference in the quadrupole splitting width between the Lo and Ld phases is much smaller than that of 24dCho, which potentially compromises the accurate measurements of the Lo/Ld partition ratios of Cho through the spectral simulations.

The 24 position is close to the side chain terminus, and thus it is expected to be located deeply in a bilayer interior. The ^{2}H NMR data of 24dCho in the PSM/Cho membrane showed a slightly smaller Δν value in comparison with that of the SSM/Cho membrane (Table 1). A similar tendency was also found in the ternary SM/DOPC/Cho membranes in mixed phase conditions at 40 °C and 50 °C (Fig. 5). These findings consistently indicate that the mobility at C24 in SSM membranes is slightly more restricted than that from PSM membranes. In terms of the lipid interaction, previous reports indicate that PSM interacts with Cho most strongly among SMs bearing various acyl-chain lengths and unsaturations.[43] On the other hand, our ^{2}H NMR results show that SSM induced wider Δν values. Thus, the difference between SSM and PSM regarding the potency of the SM-Cho interactions cannot be directly related to the different Δν values of 24dCho. On the other hand, it has been reported that the lipid chain order becomes highest at the middle of a leaflet in the presence of Cho and gradually decreases as the position of ^{2}H-lebeling moves down to the leaflet interface.[36,55] Therefore, the slightly higher mobility at the C24 position of Cho in PSM/Cho bilayers indicates that the side chain of Cho resides a little closer to the leaflet interface. Previously, X-ray diffraction studies revealed that the P-P distances of SSM unitary bilayers (52.0 Å) and SSM/Cho 50:50 bilayers (46.6 Å) were thicker than PSM unitary bilayers (49.6 Å) and PSM/Cho 50:50 bilayers (45.2 Å), respectively.[56,57] Similar observations by MD simulations were reported for binary SSM/Cho bilayers, where a 1–2 Å thicker bilayer than that of the PSM/Cho bilayer was observed.[58] The molecular axis of Cho is known to be directed mostly in parallel to the bilayer normal,[59] thus the small tilt angle difference of the Cho's sterol core in PSM (15.9° at 45 °C) and SSM (14.6° at 50 °C)[58] negligibly affects the membrane thickness (～0.1 Å). Therefore, the observed difference in the Δν values implies that the C24 of Cho in the

PSM bilayer is somewhat closer to the leaflet interface because the acyl chain of PSM is shorter, which makes the PSM bilayers thinner than those of SSM. Therefore, 24dCho can report the relative membrane depth of the Cho side chain from the leaflet interface based on its Δν values.

Although the structural difference between SSM and PSM is only two methylene units in the acyl chain, Cho is about 10 mol% more partitioned to the Lo phase consisting of SSM rather than that of PSM (Fig. 6). A previous report has revealed that Cho or its fluorescent probe CTL preferred PSM over any other saturated SMs, including SSM in a ternary SM/POPC/Cho membrane.[43] On the other hand, SSM is less miscible with DOPC than PSM, thus having a substantial effect on the gel phase formation in the binary SSM/DOPC bilayer.[60] Therefore, it is speculated that the SSM largely segregated from DOPC possibly forms larger Lo domains to which Cho partitions more preferentially regardless of intermolecular interactions between SM and Cho. These findings may partly account for the distinctive distributions of SSM and PSM in mammalian tissues and cells.[32] Because the abundance of Cho in each cell membrane is sufficient and mammalian cells contain a significant amount of SMs with C16 and C18 acyl chains in different ratios,[31] it is also assumed that the dynamics of the microdomain structure may partly be regulated by the contents of SSM and PSM.

In comparison with widely used 3dCho, 24dCho showed a significantly larger difference in the Pake doublet widths between the Lo and Ld phases. Therefore, 24dCho would be more useful than 3dCho in determining the distribution ratios of Cho for diverse phase-segregated membrane systems. The probe may also facilitate the elucidation of Cho-lipid interactions as well as Cho distributions and properties in biological membranes using ^{2}H NMR, such as the plasma membrane, micro vesicles, and exosome

membranes.

Conclusion

A new Cho probe, 24dCho, was developed for solid state ^{2}H NMR to determine the Cho-lipid interactions and the distribution and partition of Cho in bilayer membranes. Efficient synthesis of 24dCho was achieved in the seven steps of transformation, including the ^{2}H-introduction at the C24(*S*) position in a highly stereoselective manner. The Cho probe sensitively reflects the ordering of the surrounding lipids and dependently altered widths of the Pake doublet in ^{2}H NMR spectra. Furthermore, the different Pake doublet widths of 24dCho in the PSM and SSM membranes demonstrate that the relative depth of the Cho position is different between these bilayers. In the SM/DOPC/Cho membrane, where the Lo and Ld phases coexist, 24dCho present in the Lo phase shows a remarkably wider doublet signal, which is clearly separated from a much narrower doublet signal in the Ld phase. The ratio of the Lo/Ld signal area directly exhibits the Cho distribution ratios, thus clearly showing a difference in the Lo/Ld partition ratios between stearoyl-SM containing and palmitoyl-SM containing membranes, which differ only by two methylene units of the SM acyl chains. Synthetic 24dCho is a useful NMR probe to elucidate Cho distributions and the physicochemical properties in model membranes, and it can be applicable to biological membranes.

Experimental

Generals: Cho and other standard chemicals were purchased from Nacalai Tesque (Kyoto, Japan). Dry solvents for organic reactions and silica gels for column chromatography (Silica gel 60N 100–210 μm and 40–50 μm) were purchased from Kanto

Chemical Co. (Tokyo, Japan). The TLC glass plate (Silica gel 60_{F254}) was purchased from Merck (Darmstadt, Germany). The deuterated solvents and deuterium depleted water for NMR experiments were obtained from CIL (Tewksbury, MA, US) and ISOTEC (St. Louis, MO, US). Solution NMR was collected by JEOL ECS-400 (400 MHz) and ECA-500 (500 MHz) spectrometers (Tokyo, Japan). The chemical shifts of ^{1}H NMR were calibrated according to the solvent signals ($CDCl_3$; 7.26 ppm and CD_3OD; 3.30 ppm). Mass spectra were collected by LTQ-Orbitrap XL with an ESI beam source (Thermo Fisher Scientific, Waltham, MA, USA). Non-labeled PSM and SSM were isolated from egg SM or brain SM (Avanti, Alabaster, AL, US) by reverse-phase HPLC (column; Cosmosil C18-AR-II, eluent; 100% MeOH). Synthetic procedures of 24dCho are described in Supporting Information.

Solid-state ^{2}H NMR: Multi-lamellar vesicles (MLV) for solid state ^{2}H NMR were prepared in a conventional manner.[13] The lipid mixtures in an appropriate lipid molar ratio were dissolved in methanol–chloroform (1:1), and an appropriate amount of Cho solution in methanol–chloroform (1:1) was combined to comprise the total lipid amount of 15 mg. The organic solvent was removed by evaporation, and the homogeneous lipid film was prepared by cycles of the dissolution and the removal of the methanol–chloroform. The film was then dried for 12 h under a high vacuum condition. The resulting lipid film was hydrated with water (30 times of the lipid weight), vortexed, and sonicated. The hydrated sample was freeze-thawed 15 times and lyophilized for at least 12 h. The lipid film was again rehydrated with deuterium-depleted water to reach 50% moisture (w/w), vortexed, and freeze-thawed several times. The sample was transferred into the NMR tube. Finally, the tube was sealed with epoxy glue.

The solid-state ^{2}H-NMR spectra were recorded on a 300 MHz or 400 MHz spectrometer (CMX-300, Varian, Palo Alto, CA, US, AVANCE400, Bruker, Billerica, Massachusetts, USA) equipped with static ^{2}H probes. A solid echo pulse sequence[61] was used with a 90° pulse width set to 2.0 μs, and the solid echo delays were set to 30 μs and 20 μs, respectively. The initial delay was set to 0.5 s. The sweep width was set to 250 kHz with 4k data points, and the number of scans was approximately 30,000. FID data were Fourier transformed upon exponential multiplication. The splitting widths of the ^{2}H signals ($\Delta\nu_{obs}$) can be expressed by the following equation:

$$\Delta\nu_{obs} = \frac{3e^2qQ}{2\ \ h} S\left(\frac{3\cos^2\theta_q - 1}{2}\right), \tag{1}$$

where e^2qQ/h is the quadrupolar coupling constant in 170 kHz of a typical methylene group, S includes the scaling and order parameters, and θ_q is the angle between the C-D vector and the outer magnetic field.

Peak fitting: The fitting of the ^{2}H NMR spectra was performed for the elliptical spheres.[62] Assuming an ellipsoidal shape of liposomes and a fast uniaxial rotation of lipid molecules, the probability density $P(\beta)$ is expressed as

$$P(\beta) = \frac{\sin\beta}{\{\sin^2\beta + (a/c)^2\cos^2\beta\}^2}\ , \tag{1}$$

where β is the angle of bilayer normal with respect to the external magnetic field, and a and c are the semi-minors and semi-major ellipse axes, respectively. Thus, the line shape of static ^{2}H NMR spectrum can be written as

$$I(\omega) = \int_0^{\pi}\{W[\omega - g_+(\beta)] + W[\omega - g_-(\beta)]\}P(\beta)d\beta \ , \quad [2]$$

where I is the signal intensity at a given frequency, ω, and W is a broadening function (Lorentzian or Gaussian). $g_+(\beta)$ and $g_-(\beta)$ are peak top positions at a given quadrupolar splitting value, $\Delta\nu$, written as

$$g_\pm(\beta) = \pm\frac{1}{2}\Delta\nu(\beta) \ . \quad [3]$$

The numerical integration of [2] was carried out from 0.25° to 89.75° by 0.5° due to the symmetric feature of these equations with respect to 90°, and the Lorentzian distribution function was used for line broadening.

Acknowledgements

The authors would like to thank Drs. N. Inazumi and Y. Todokoro (Osaka University) for their assistance in the NMR measurements and Prof. J. Peter Slotte (Åbo Akademi University) for the discussion. This work was supported by the Grants-in-Aids for Scientific Research (S) 16H06315, (C) 19K05713, for "Frontier Research on Chemical Communications" 17H06406 from the Japan Society for the Promotion of Science, and JST CREST Grant Number JPMJCR18H2.

Conflict of Interest

The authors declare no conflict of interest.

Supporting Information

Supporting information for this article is provided via a link at the end of the document.

Author Information

Corresponding Authors

*E-mail: hanashimas13@chem.sci.osaka-u.ac.jp (S.H.); murata@chem.sci.osaka-u.ac.jp (M.M.).

References

1 K. Simons and E. Ikonen, *Nature*, 1997, **387**, 569–572.

2 D. A. Brown and E. London, *Annu. Rev. Cell Dev. Biol.*, 1998, **14**, 111–136.

3 M. Kinoshita, K. G. Suzuki, N. Matsumori, M. Takada, H. Ano, K. Morigaki, M. Abe, A. Makino, T. Kobayashi, K. M. Hirosawa, T. K. Fujiwara, A. Kusumi and M. Murata, *J. Cell Biol.*, 2017, **216**, 1183–1204.

4 F. R. Maxfield and G. van Meer, *Curr. Opin. Cell Biol.*, 2010, **22**, 422–429.

5 B. Ramstedt and J. P. Slotte, *Biochim. Biophys. Acta*, 2006, **1758**, 1945–1956.

6 E. Ikonen, *Nat. Rev. Mol. Cell Biol.*, 2008, **9**, 125–138.

7 N. Matsumori, T. Yasuda, H. Okazaki, T. Suzuki, T. Yamaguchi, H. Tsuchikawa, M. Doi, T. Oishi and M. Murata, *Biochemistry*, 2012, **51**, 8363–8370.

8 Y. Yano, S. Hanashima, T. Yasuda, H. Tsuchikawa, N. Matsumori, M. Kinoshita, M. A. Al Sazzad, J. P. Slotte and M. Murata, *Biophys. J.*, 2018, **115**, 1530–1540.

9 J. Huang and G. W. Feigenson, *Biophys. J.*, 1999, **76**, 2142–2157.

10 S. Endapally, D. Frias, M. Grzemska, A. Gay, D. R. Tomchick and A. Radhakrishnan, *Cell*, 2019, **176**, 1040–1053.

11 T. Kishimoto, R. Ishitsuka and T. Kobayashi, *Biochim. Biophys. Acta*, 2016, **1861**, 812–829.

12 T. Tomita, K. Noguchi, H. Mimuro, F. Ukaji, K. Ito, N. Sugawara-Tomita and Y. Hashimoto, *J. Biol. Chem.*, 2004, **279**, 26975–26982.

13 T. K. M. Nyholm, S. Jaikishan, O. Engberg, V. Hautala and J. P. Slotte, *Biophys. J.*, 2019, **116**, 296–307.

14 P. L. Yeagle, *Biochim. Biophys. Acta*, 1985, **822**, 267–287.

15 A. A. Waheed, Y. Shimada, H. F. Heijnen, M. Nakamura, M. Inomata, M. Hayashi, S. Iwashita, J. W. Slot and Y. Ohno-Iwashita, *Proc. Natl. Acad. Sci. USA*, 2001, **98**, 4926–4931.

16 M. Holtta-Vuori, R. L. Uronen, J. Repakova, E. Salonen, I. Vattulainen, P. Panula, Z. Li, R. Bittman and E. Ikonen, *Traffic*, 2008, **9**, 1839–1849.

17 O. Behnke, J. Tranum-Jensen and B. van Deurs, *Eur. J. Cell Biol.*, 1984, **35**, 200–215.

18 L. M. Loura, A. Fedorov and M. Prieto, *Biochim. Biophys. Acta*, 2001, **1511**, 236–243.

19 F. S. Ariola, Z. Li, C. Cornejo, R. Bittman and A. A. Heikal, *Biophys. J.*, 2009, **96**, 2696–2708.

20 M. Kozorog, M. A. Sani, F. Separovic and G. Anderluh, *Chem. Eur. J.,* 2018, **24**, 14220–14225.

21 A. Cruz, L. Vazquez, M. Velez and J. Perez-Gil, *Langmuir*, 2005, **21**, 5349–5355.

22 F. R. Maxfield and D. Wustner, *Methods Cell Biol.*, 2012, **108**, 367–393.

23 M. Mondal, B. Mesmin, S. Mukherjee and F. R. Maxfield, *Mol. Biol. Cell*, 2009, **20**, 581–588.

24 A. Bjorkbom, B. Ramstedt and J. P. Slotte, *Biochim. Biophys. Acta Biomembr.*, 2007, **1768**, 1839–1847.

25 J. R. Robalo, A. M. do Canto, A. J. Carvalho, J. P. Ramalho and L. M. Loura, *J. Phys. Chem. B*, 2013, **117**, 5806–5819.

26 L. J. Nabo, N. H. List, S. Witzke, D. Wustner, H. Khandelia and J. Kongsted, *Biochim. Biophys. Acta*, 2015, **1848**, 2188–2199.

27 H. A. Scheidt, P. Muller, A. Herrmann and D. Huster, *J. Biol. Chem.*, 2003, **278**, 45563–45569.

28 C. M. McQuaw, L. Zheng, A. G. Ewing and N. Winograd, *Langmuir*, 2007, **23**, 5645–5650.

29 H. Ogiso, M. Taniguchi and T. Okazaki, *J. Lipid Res.*, 2015, **56**, 1594–1605.

30 A. Llorente, T. Skotland, T. Sylvanne, D. Kauhanen, T. Rog, A. Orlowski, I. Vattulainen, K. Ekroos and K. Sandvig, *Biochim. Biophys. Acta*, 2013, **1831**, 1302–1309.

31 T. Sassa and A. Kihara, *Biomol. Ther.*, 2014, **22**, 83–92.

32 A. Kihara, *J. Biochem.*, 2012, **152**, 387–395.

33 R. Tidhar and A. H. Futerman, *Biochim. Biophys. Acta*, 2013, **1833**, 2511–2518.

34 M. Sugimoto, Y. Shimizu, T. Yoshioka, M. Wakabayashi, Y. Tanaka, K. Higashino, Y. Numata, S. Sakai, A. Kihara, Y. Igarashi and Y. Kuge, *Biochim. Biophys. Acta Mol. Cell Biol. Lipids*, 2015, **1851**, 1554–1565.

35 N. Matsumori, H. Okazaki, K. Nomura and M. Murata, *Chem. Phys. Lipids*, 2011, **164**, 401–408.

36 T. Bartels, R. S. Lankalapalli, R. Bittman, K. Beyer and M. F. Brown, *J. Am. Chem. Soc.*, 2008, **130**, 14521–14532.

37 T. Yasuda, H. Tsuchikawa, M. Murata and N. Matsumori, *Biophys. J.*, 2015, **108**, 2502–2506.

38 J. Cui, S. Lethu, T. Yasuda, S. Matsuoka, N. Matsumori, F. Sato and M. Murata, *Bioorg. Med. Chem. Lett.*, 2015, **25**, 203–206.39 R. Malabed, S. Hanashima, M. Murata and K. Sakurai, *Biochim. Biophys. Acta Biomembr*, 2017, **1859**, 2516–2525.

40 J. J. Kinnun, R. Bittman, S. R. Shaikh and S. R. Wassall, *Biophys. J.*, 2018, **114**, 380–391.

41 R. Murari, M. P. Murari and W. J. Baumann, *Biochemistry*, 1986, **25**, 1062–1067.

42 A. Vogel, H. A. Scheidt, D. J. Baek, R. Bittman and D. Huster, *Phys. Chem. Chem. Phys.*, 2016, **18**, 3730–3738.

43 S. Jaikishan and J. P. Slotte, *Biochim. Biophys. Acta*, 2011, **1808**, 1940–1945.

44 R. Martin, E. V. Entchev, F. Dabritz, T. V. Kurzchalia and H. J. Knolker, *Eur. J. Org. Chem.*, 2009, 3703–3714.

45 M. M. Midland, *Chem. Rev.*, 1989, **89**, 1553–1561.

46 I. Ohtani, T. Kusumi, Y. Kashman and H. Kakisawa, *J. Am. Chem. Soc.*, 1991, **113**, 4092–4096.

47 S. Li, J. Pang, W. K. Wilson and G. J. Schroepfer, Jr., *Chem. Phys. Lipids*, 1999, **99**, 33–71.

48 Y. Nishida, H. Uzawa, S. Hanada, H. Ohrui H. Meguro, *Agric. Biol. Chem.* 1989, **53**, 2319–2326.

49 M. R. Krause and S. L. Regen, *Acc. Chem. Res.*, 2014, **47**, 3512–3521.

50 T. Yasuda, N. Matsumori, H. Tsuchikawa, M. Lonnfors, T. K. Nyholm, J. P. Slotte and M. Murata, *Langmuir*, 2015, **31**, 13783–13792.

51 D. Marsh, *Biochim. Biophys. Acta*, 2010, **1798**, 688–699.

52 R. Koynova and M. Caffrey, *Biochim. Biophys. Acta*, 1995, **1255**, 213–236.

53 T. K. Nyholm, D. Lindroos, B. Westerlund and J. P. Slotte, *Langmuir*, 2011, **27**, 8339–8350.

54 S. L. Veatch and S. L. Keller, *Phys. Rev. Lett.*, 2005, **94**, 148101.

55 T. Yasuda, M. Kinoshita, M. Murata and N. Matsumori, *Biophys. J.*, 2014, **106**, 631–638.

56 P. R. Maulik and G. G. Shipley, *Biochemistry*, 1996, **35**, 8025–8034.

57 P. R. Maulik and G. G. Shipley, *Biophys. J.*, 1996, **70**, 2256–2265.

58 E. Wang and J. B. Klauda, *J. Phys. Chem. B*, 2017, **121**, 4833–4844.

59 W. F. Bennett, J. L. MacCallum, M. J. Hinner, S. J. Marrink and D. P. Tieleman, *J. Am. Chem. Soc.*, 2009, **131**, 12714–12720.

60 A. Kullberg, O. O. Ekholm and J. P. Slotte, *Biophys. J.*, 2015, **109**, 1907–1916.

61 J. H. Davis, K. R. Jeffrey, M. Bloom, M. I. Valic and T. P. Higgs, *Chem. Phys.*

Lett., 1976, **42**, 390–394.

62 T. Pott and E. J. Dufourc, *Biophys. J.*, 1995, **68**, 965–977.